Yuan et al. *Zool. Res.* 2023, 44(2): 303−314
https://doi.org/10.24272/j.issn.2095-8137.2022.384

ZR | Zoological Research

Article Open Access

A 1.1 Mb duplication CNV on chromosome 17 contributes to skeletal muscle development in Boer goats

Ying Yuan[1,2,#], Wei-Yi Zhang[1,2,#], Bai-Gao Yang[1,2], Dong-Ke Zhou[1,2], Lu Xu[1,2], Yong-Meng He[1,2], Hao-Yuan Zhang[1,2], Cheng-Li Liu[1,2], Yue-Hui Ma[3], Ming-Xing Chu[3], Wen-Guang Zhang[4], Hui-Jiang Gao[3], Lin Jiang[3], Fu-Ping Zhao[3], Lu-Pei Zhang[3], Ri-Su Na[4], Baatarchogt Oyungerel[5], Yan-Guo Han[1,2], Yan Zeng[1,2], Shi-Zhi Wang[1,2], Huai-Zhi Jiang[6], Hong-Ping Zhang[7], Xun-Ping Jiang[8], Jian-Ning He[9], Hao Liang[10], Kaushalendra Kaushalendra[11], Ya-Wang Sun[1,2], Yong-Fu Huang[1,2], Yong-Ju Zhao[1,2], Zhong-Quan Zhao[1,2], Guang-Xin E[1,2,*]

[1] *College of Animal Science and Technology*, *Southwest University*, *Chongqing* 400715, *China*
[2] *Chongqing Key Laboratory of Forage & Herbivore*, *Chongqing* 400715, *China*
[3] *Institute of Animal Science*, *Chinese Academy of Agricultural Sciences (CAAS)*, *Beijing* 100193, *China*
[4] *College of Animal Science*, *Inner Mongolia Agricultural University*, *Huhhot*, *Inner Mongolia* 010018, *China*
[5] *School of Animal Science & Biotechnology*, *Mongolian University of Life Sciences*, *Zaisan*, *Khan-uul*, *Ulaanbaatar* 17024, *Mongolia*
[6] *Animal Science and Technology College*, *Jilin Agriculture University*, *Changchun*, *Jilin* 130118, *China*
[7] *Farm Animal Genetic Resources Exploration and Innovation Key Laboratory of Sichuan Province*, *College of Animal Science and Technology*, *Sichuan Agricultural University*, *Chengdu*, *Sichuan* 611130, *China*
[8] *Key Lab of Agricultural Animal*, *Genetics*, *Breeding and Reproduction of Ministry of Education*, *College of Animal Science and Technology*, *Huazhong*, *Agricultural University*, *Wuhan*, *Hubei* 430070, *China*
[9] *College of Animal Science and Technology*, *Qingdao Agricultural University*, *Qingdao*, *Shandong* 266109, *China*
[10] *State Key Laboratory of Reproductive Regulation and Breeding of Grassland Livestock*, *School of Life Sciences*, *Inner Mongolia University*, *Hohhot*, *Inner Mongolia* 010070, *China*
[11] *Department of Zoology*, *Pachhunga University College*, *Mizoram University*, *Aizawl* 796001, *India*

ABSTRACT

The Boer goat is one of the top meat breeds in modern animal husbandry and has attracted widespread attention for its unique growth performance. However, the genetic basis of muscle development in the Boer goat remains obscure. In this study, we identified specific structural variants in the Boer goat based on genome-wide selection signals and analyzed the basis of the molecular heredity of related candidate genes in muscle development. A total of 9 959 autosomal copy number variations (CNVs) were identified through selection signal analysis in 127 goat genomes. Specifically, we confirmed that the highest signal CNV (HSV) was a chromosomal arrangement containing an approximately 1.11 Mb (CHIR17: 60062304–61171840 bp) duplicated fragment inserted in reverse orientation and a 5 362 bp deleted region (CHIR17:60145940–60151302 bp) with overlapping genes (e.g., *ARHGAP10*, *NR3C2*, *EDNRA*, *PRMT9*, and *TMEM184C*). The homozygous duplicated HSV genotype (+/+) was found in 96% of Boer goats but was not detected in Eurasian goats and was only detected in 4% of indigenous African goats. The expression network of three candidate genes (*ARHGAP10*, *NR3C2*, and *EDNRA*) regulating dose transcription was constructed by RNA sequencing. Results indicated that these genes were involved in the proliferation and differentiation of skeletal muscle satellite cells (SMSCs) and their overexpression significantly increased the expression of *SAA3*. The HSV of the Boer goat contributed to superior skeletal muscle growth via the dose effects of overlapping genes.

Keywords: Boer goat; CNV; Muscle development; SMSCs

INTRODUCTION

Boer goat is a world-renowned meat breed of goat characterized by a large body and good meat production. Because of its broad ecological adaptability, it has been widely introduced in many countries for the hybrid genetic improvement of native goats (Marques et al., 2021; Ncube

Received: 25 November 2022; Accepted: 06 February 2023; Online: 07 February 2023
Foundation items: This work was supported by the National Natural Science Foundation of China (32272834)
[#]Authors contributed equally to this work
*Corresponding author, E-mail: eguangxin@126.com

et al., 2022; Pérez-Baena et al., 2021). Many researchers have explored its meat quality (van Wyk et al., 2022), feeding mode (Pérez-Baena et al., 2021), and reproductive performance (Bezerra et al., 2019; Kholif et al., 2020), as well as the molecular basis of muscle development, coat color, and environmental adaptation (Chaosap et al., 2020; Shakweer & El-Rahman, 2020; Wang et al., 2019b; Xiong et al., 2020). However, the genetic basis for its superior muscle growth remains poorly understood.

Copy number variation (CNV) is a major form of genomic structural variation, defined as the deletion/duplication of genomic fragments of more than 1 kb caused by genome rearrangements (Xie & Tammi, 2009). CNVs participate in various biological functions and phenotype formation through the dosage effects of included genes and are involved in the reconstruction of gene regulatory regions (Pielberg et al., 2003; Shen et al., 2013; Xu et al., 2020). For example, *CCL3L1* copy exhibits a robust large-scale gene dosage effect on *CCL3L1* mRNA levels (Adewoye et al., 2018). The human *SLC2A3* gene locus located on chromosome 12p13.31 is unstable and prone to non-allelic homologous recombination events, generating multiple CNVs of *SLC2A3* that alter *SLC2A3* expression (Veal et al., 2014). Specifically, organ development, proliferation, and cellular degeneration are particularly susceptible to *SLC2A3* copy number alterations (Ziegler et al., 2020). Furthermore, the 16p11.2 and 22q11.2 genes involved in CNVs are thought to have copy number dose-dependent effects on the behavior of affected humans (Shishido et al., 2014). Overall, CNVs are closely related to the expression levels of the covered genes and the copy numbers of most genes are positively correlated with their expression (Shao et al., 2019). Recent studies have suggested that CNVs are key drivers of phenotypic diversity and economic traits in domesticated animals (Ladeira et al., 2022; Lye & Purugganan, 2019; Paudel et al., 2013), and are associated with goat muscle development (Huang et al., 2021; Liu et al., 2019).

Skeletal muscle is the main source of protein in edible meat (Yin et al., 2020), and its developmental status directly determines the growth-related economic traits of animals (Dodson et al., 2010). The formation of new muscle fibers in skeletal muscle depends on the activation of muscle-specific precursor cells (Dumont et al., 2015; Relaix & Zammit, 2012). The self-renewal and proliferation of skeletal muscle satellite cells (SMSCs) can provide many myogenic cells, which redifferentiate into myoblasts and fuse into myotubes to form new muscle fibers (Chang & Rudnicki, 2014).

The development of SMSCs is a complex process due to the co-regulation of numerous signaling pathways and genes (Giordani et al., 2018; Milewska et al., 2014). In recent decades, the genetic basis of goat skeletal muscle development has been investigated. Studies have shown that the *MSTN* gene is a negative regulator of skeletal muscle growth and development and functions by controlling the number, size, and type of muscle fibers (Bi et al., 2021). *GSK3β* regulates the expression of the *MYHC-2A* gene via *NFATC2* to promote SMSC differentiation in goats (Wang et al., 2019a). The mTOR signaling pathway regulates the phosphorylation of myocyte enhancer factor 2 (*MEF2*) through *ILK*, thereby affecting SMSC proliferation and differentiation (Wu et al., 2015).

In this study, we aimed to identify CNVs and high-frequency dominant genotypes associated with the extraordinary economic phenotypes in Australian Boer goats via genome-wide selection signal analysis. We also clarified the molecular roles of candidate genes carried by the variants in the proliferation and differentiation of SMSCs and the dose effect-based expression regulation of downstream genes.

MATERIALS AND METHODS

Genome-wide sequencing and selection signal analysis of CNV dataset

All applicable international, national, and institutional guidelines for the care and use of animals were strictly followed. All animal collection protocols complied with the current laws of China. The experimental protocols were approved by the Animal Care Committee of Southwest University (Permit No. IACUC-20210415-04) in compliance with the recommendations of the Regulations for the Administration of Affairs Concerning Experimental Animals of China.

A total of 127 publicly available goat genome datasets were downloaded from the NCBI Sequence Read Archive (SRA), including 46 Australian Boer goats from our previous study (Yang et al., 2021) and 81 other goats (45 African, 16 European, and 20 Asian goats) as the control group (Supplementary Table S1).

The raw genomic data were trimmed and filtered using Trimmomatic software (v0.36). High-quality clean reads were mapped to the goat reference genome (ARS1, GCF_001704415.1) using BWA-MEM (v0.7.17-r1188) with default parameters. Potential polymerase chain reaction (PCR) duplicates were removed by Picard (http://broadinstitute.github.io/picard). CNVcaller (Wang et al., 2017b) was used to determine CNVs, retaining those with silhouette score>0.65 and minor allelic frequency (MAF)>0.05 to prevent possible false positives. Selective sweep analysis of CNVs was performed with V_{ST} and F_{ST}. Variants were annotated by ANNOVAR (ANNOate VARiation). Candidate genes were identified and annotated from the top 20 CNVs using the V_{ST} and F_{ST} indices. Candidate genes were also annotated based on Gene Ontology (GO) and Kyoto Encyclopedia of Genes and Genomes (KEGG) analyses using the online tool KOBAS (http://kobas.cbi.pku.edu.cn/kobas3) with corrected P<0.05 as the threshold for significant enrichment.

To further explore the genotype frequencies of key candidate CNVs in Chinese indigenous goat populations, we followed the above-mentioned CNV identification methods to supplement the CNV genotypes of four indigenous breeds in southwest China (20 Dazu black goats, 20 Youzhou black goats, 20 Hechuan white goats, and 20 Hainan goats) (Supplementary Table S2). Venous blood samples (1.5 mL) were collected, and genomic DNA was extracted using a DNeasy Blood & Tissue Kit (Qiagen, Germany). DNA libraries were constructed with an Illumina NGS Fast DNA Library Prep Set Illumina Kit (Illumina, USA). The genome of each animal was sequenced using the Illumina NovaSeq 6000 system for 10× sequencing (BGI, China). All bioinformatics analysis steps were performed as described above.

Exploration of candidate CNV structures using long-read genome-wide sequencing and PCR-Sanger sequencing

One DNA sample was collected from each of the 46 Australian Boer goats. A SMRT bell CLR library was constructed using a Pacific Biosciences SMRTbell Express Template Prep Kit 2.0.

The constructed libraries were size-selected on a BluePippin™ system for molecules ≥25 kb and subjected to primer annealing. The SMRTbell templates were bound to polymerases using a DNA/Polymerase Binding Kit. Sequencing was carried out using the Pacific Bioscience Sequel platform (PacBio, USA).

To verify the structural variant genotypes of chromosomal rearrangements, PCR primers (Supplementary Table S3) targeting breakpoints based on an approximately 1.11 Mb chromosomal rearrangement (CHIR17:60062304–61171840) were designed using the Primer (v3.04) online tool (http://bioinfo.ut.ee/primer3-0.4.0/). For PCR amplification, 2×TransTaq® High Fidelity (HiFi) PCR SuperMix II (TransGen Biotech, China) was used. The PCR conditions consisted of initial denaturation at 94 °C for 5 min, followed by 35 cycles of denaturation at 94 °C for 30 s, annealing at locus-specific annealing temperature (Tm) for 30 s, and extension at 72 °C for 2 min, with a final extension at 72 °C for 7 min. Sanger sequencing was conducted using two methods on the ABI 3730 sequencing platform (Life Technologies, USA).

Culture and identification of SMSCs in goats

First, 3 cm^3 leg muscle samples were obtained from 1-month-old Dazu black goats. After removing fat and connective tissues, the muscles were digested with 0.1% type I collagenase (Solarbio, China) and 0.25% trypsin (HyClone, USA) to release the cells. The SMSC suspension was filtered and detached, after which the cells were cultured 10% growth medium (GM) containing Dulbecco's Modified Eagle Medium (DMEM/F; Thermo Fisher Scientific, China), 10% fetal bovine serum (Thermo Fisher Scientific, China), and 2% penicillin/streptomycin (Invitrogen, USA) at 37 °C in a humidified atmosphere of 5% CO_2. Differentiated SMSCs were induced using differentiation medium (DM) containing DMEM and 2% horse serum (HyClone, USA) when their density reached 70%–80% in the GM. Immunofluorescence staining of Pax7 was performed to identify SMSC purity (Feng et al., 2018), and Pax7 monoclonal rabbit antibodies were provided by Absin (China).

Candidate gene overexpression vector construction and transfection into SMSCs

To identify effects on SMSC proliferation and differentiation, lentiviral vectors (HBLV-*ARHGAP10*-3xflag-ZsGreen-PUR, HBLV-*EDNRA*-HIS-mCherry-BSD, and HBLV-*NR3C2*-3xflag-ZsGreen-PURO; HANBIO, China) expressing flag-tagged *ARHGAP10* (Gene ID: 102173323), *EDNRA* (Gene ID: 102174144), and *NR3C2* (Gene ID: 102172834) were first constructed. Their cDNAs were synthesized by PCR amplification with corresponding primer pairs (Supplementary Table S4) and inserted between the EcoRI and BamHI sites. HBLV-ZsGreen-PURO and HBLV-mCherry-BSD empty vectors were used as negative controls. Lentiviral transfection was performed when SMSC density reached 60%–70%. Transfection efficiency was assessed based on cell fluorescence using a fluorescence microscope (Leica DMi8, Germany) after 48 h.

At 12, 24, 36, and 72 h after transfection of overexpressed candidate genes into the SMSCs, cell proliferation was measured using a CCK8 Kit (Solarbio, China) by recording absorbance at 450 nm and running three parallel replicates. At 48 h after transfection, an EdU (5-ethynyl-2'-deoxyuridine) experiment was performed using a C10310 EdU Apollo *In Vitro* Imaging Kit (Ribobio, China). At least four fields were randomly selected to observe the number of stained cells under a fluorescence microscope (Leica DMi8, Germany).

To identify SMSC differentiation when candidate genes were overexpressed, we carried out lentiviral transfection, followed by cell culture for 36 h at 37 °C. SMSC differentiation was induced for 4 days by switching from GM to DM. Total RNA was extracted using RNAiso Plus (Solarbio, China). The mRNA expression levels of myogenic differentiation marker genes (*MyoD*, *MyoG*) were measured by quantitative real-time PCR (qRT-PCR) (Metzger et al., 2020).

Molecular regulatory network investigation of overexpressed candidate genes in SMSCs by RNA sequencing (RNA-seq)

The SMSC sample settings for RNA-seq were: *ARHGAP10* overexpressed group (AA) and its no-load control (AO); *EDNRA* overexpression group (EA) and its no-load control (EO); and *NR3C2* overexpression group (NA) and its no-load control (NO). Three biological replicates were established for each group. Total RNA was extracted using a Trizol Reagent Kit (Invitrogen, USA). RNA quality was assessed with an Agilent 2100 Bioanalyzer (Agilent Technologies, USA). RNA-seq cDNA libraries were constructed using a NEBNext Ultra RNA Library Prep Kit (NEB #7530, New England Biolabs, USA). Sequencing was performed on the Illumina NovaSeq 6000 system (BGI, China).

Fastp (v0.18.0) was used to filter raw data (PRJNA843937) to obtain clean reads. The short-read alignment tool Bowtie2 (v2.2.8) was used to map the reads to the ribosomal RNA (rRNA) database. The rRNA-mapped reads were then removed. Paired-end clean reads were mapped to the reference genome (ARS1, GCA_001704415.1) using HISAT (v2.2.4) with default parameters. The mapped reads of each group were assembled using StringTie (v1.3.1) in a reference-based approach. For each transcription region, fragments per kilobase of transcripts per million mapped reads (FPKM) values were calculated to quantify expression abundance using RSEM software (Li & Dewey, 2011). Differential gene expression was analyzed by DESeq2 (Love et al., 2014). Genes with a false discovery rate (FDR)<0.05 and absolute fold-change≥2 were considered as significant differentially expressed genes (DEGs).

Bioinformatics analysis accuracy based on RNA-seq data was verified using a CFX96-Touch™ Real-Time PCR Detection system (Bio-Rad, USA). All RNA samples used for qRT-PCR were the same as those used for RNA-seq. The cDNA was synthesized using a First-Strand cDNA Synthesis Kit (Takara Bio, RR047A, China). Primer Premier 6 (Premier Biosoft, USA) was used to design the primers for the genes (Supplementary Table S5).

For qRT-PCR amplification, in accordance with the manufacturer's instructions, the reaction volume (20 μL) contained 10 μL of 2×SYBR Green PCR Master Mix (Takara Bio, China), 20 ng of cDNA, 0.5 μL (10 mmol/L) of each primer, and ddH_2O to the final volume. The qRT-PCR amplification system included: one cycle at 95 °C for 3 min, followed by 40 cycles at 95 °C for 10 s and 55 °C for 30 s. Within the runs, the samples were assayed in triplicate, and the maximum acceptable standard deviation of the threshold cycle (CT) was 0.2. Each qRT-PCR run was repeated at least three times. Glyceraldehyde 3-phosphate dehydrogenase (*GAPDH*) was used to normalize gene expression (reference gene). The relative expression levels of different qRT-PCR data were analyzed using the $2^{-\Delta\Delta Ct}$ method (Livak &

Schmittgen, 2001). Statistical analysis of relative mRNA expression was carried out using SPSS v19.0 (SPSS, USA).

RESULTS

Genome-wide selection signal analysis of CNVs in Boer goat

In this study, 9 959 CNVs were obtained on the autosomes of 127 goats. Twenty overlapping CNVs were screened according to the top 1% selection signals of the two parameters (F_{ST}≥0.430998, V_{ST}≥0.597069727; Figure 1A). A total of 23 candidate genes (e.g., *EDNRA*, *CYBA*, and *PBRM1*) were identified from those CNVs (Supplementary Table S6).

Eleven of the 23 candidate genes were enriched in 33 KEGG signaling pathways (Figure 1B; Supplementary Table S7), including growth and development-related pathways (such as osteoclast differentiation (*CYBA*)), metabolism-related signaling pathways (inositol phosphate metabolism (*PLCH2*) and metabolic pathways (*PLCH2*, *NDST3*, and *MVD*)), and biological regulatory function-related signaling pathways (MAPK signaling pathway (*CACNA1B*)). Moreover, 21 of the candidate genes were enriched to 238 GO terms (Figure 1C; Supplementary Table S8), of which 56 were significantly enriched (corrected P<0.05). According to the classification results, three GO terms were related to muscle contraction function, including artery smooth muscle contraction (*EDNRA*), smooth muscle contraction (*EDNRA*), and positive regulation of smooth muscle cell proliferation (*CYBA*). Some GO terms related to growth and development were also enriched, such as positive regulation of endothelial cell proliferation (*CYBA*), neural crest cell development (*EDNRA*), and mitotic cell cycle (*PBRM1*). Other GO terms were related to immune function (positive regulation of phagocytosis (*CYBA*)) and reproduction (oogenesis (*KMT2D*) and *in utero* embryonic development (*EDNRA*)).

Precise structure of key candidate CNVs in Boer goats

The two CNVs with the highest signal values (CNV1: F_{ST}=0.918858, V_{ST}=0.855420854, CHIR17:60062001–60297500 bp; CNV2: F_{ST}=0.918858, V_{ST}=0.877347065, CHIR17:60301001–61018500 bp) contained five coding genes (*ARHGAP10*, *NR3C2*, *EDNRA*, *TMEM184C*, and *PRMT9*). The full length of the duplication CNVs (CNV1 and CNV2) on CHIR17 was approximately 1.11 Mb, as determined by the Integrative Genome Viewer (IGV) with short reads. We confirmed that the two CNVs were seamlessly unified (HSV; Figure 2A), that is, they did not include at 4 145 bp spacer sequence, as determined by long-read and PCR-Sanger sequencing of homozygous individuals. Average read coverage of the different HSV genotypes (Figure 2B) and frequency of the HSV genotypes within populations located in different geographic areas were determined. The homozygous duplication (+/+) genotype was found in 96% of the Boer goats, 4% of the indigenous African goats, and none of the Eurasian goats (Figure 2C).

Long reads sequenced from a homozygous individual with HSV (+/+) were used for HSV structural analysis. First, a 5 363 bp (CHIR17:60145940–60151302 bp) region was observed within the 1.11 Mb HSV region of the homozygous HSV (+/+) individual without an extra copy (Figure 2D). In addition, many reads mapped to the two edges of the HSV were reverse-mapped to the outer edges of the region (CHIR17:60145940–60151302 bp), as observed by IGV. In detail, more than 80% of reads mapped to CHIR17:60137768–60145940 bp were also reversely located in the CHIR17:61167664–61171840 region (Figure 2D), and a high frequency of reads were mapped to both CHIR17:60062304–60063156 and CHIR17:60151302–60153676 in opposite

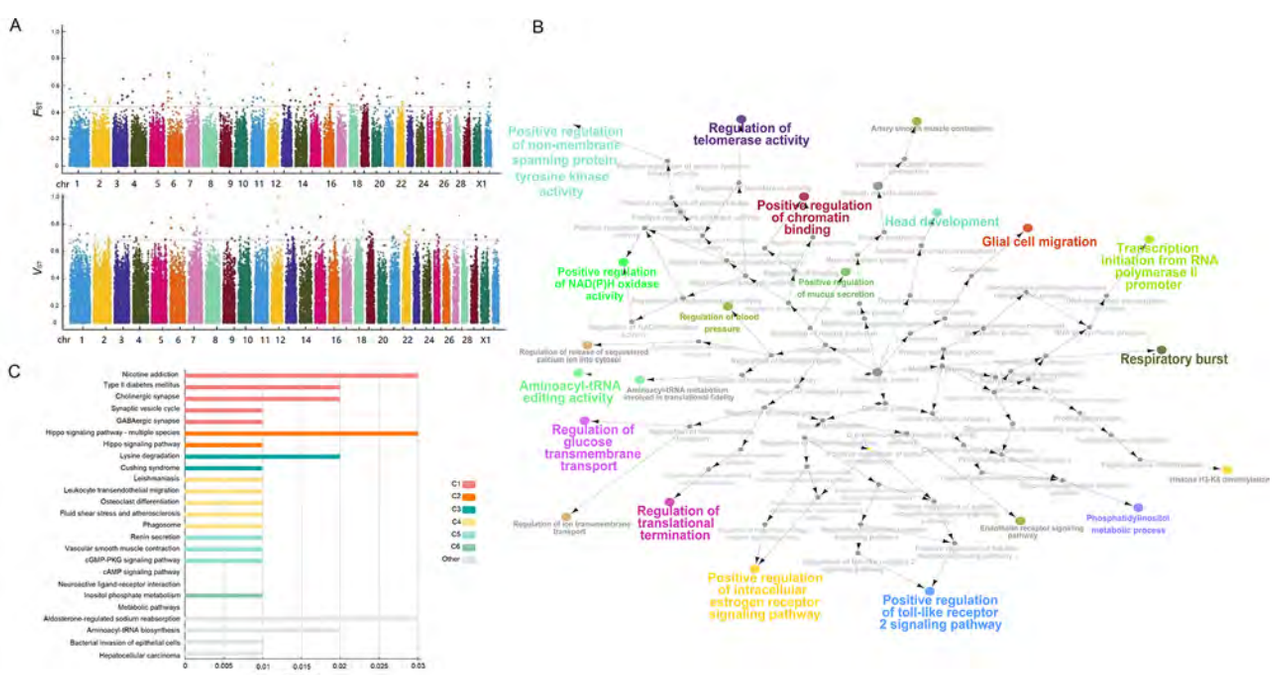

Figure 1 Genome-wide selective sweep analysis of Boer goats based on CNVs

A: Manhattan plot of F_{ST} and V_{ST} showing CNV-based selection signals of 46 Boer goats in comparison to 81 non-meat goats and top 1% of intersections of sweep windows between F_{ST} and V_{ST}. B: KEGG pathways enriched in 11 candidate genes, with top 20 intersections of selection signal parameters. C: GO network enriched in 21 candidate genes, with top 20 overlapping CNVs of two selection signal parameters. Different colors represent different biological function classifications, and size is determined by amount of GO enrichment.

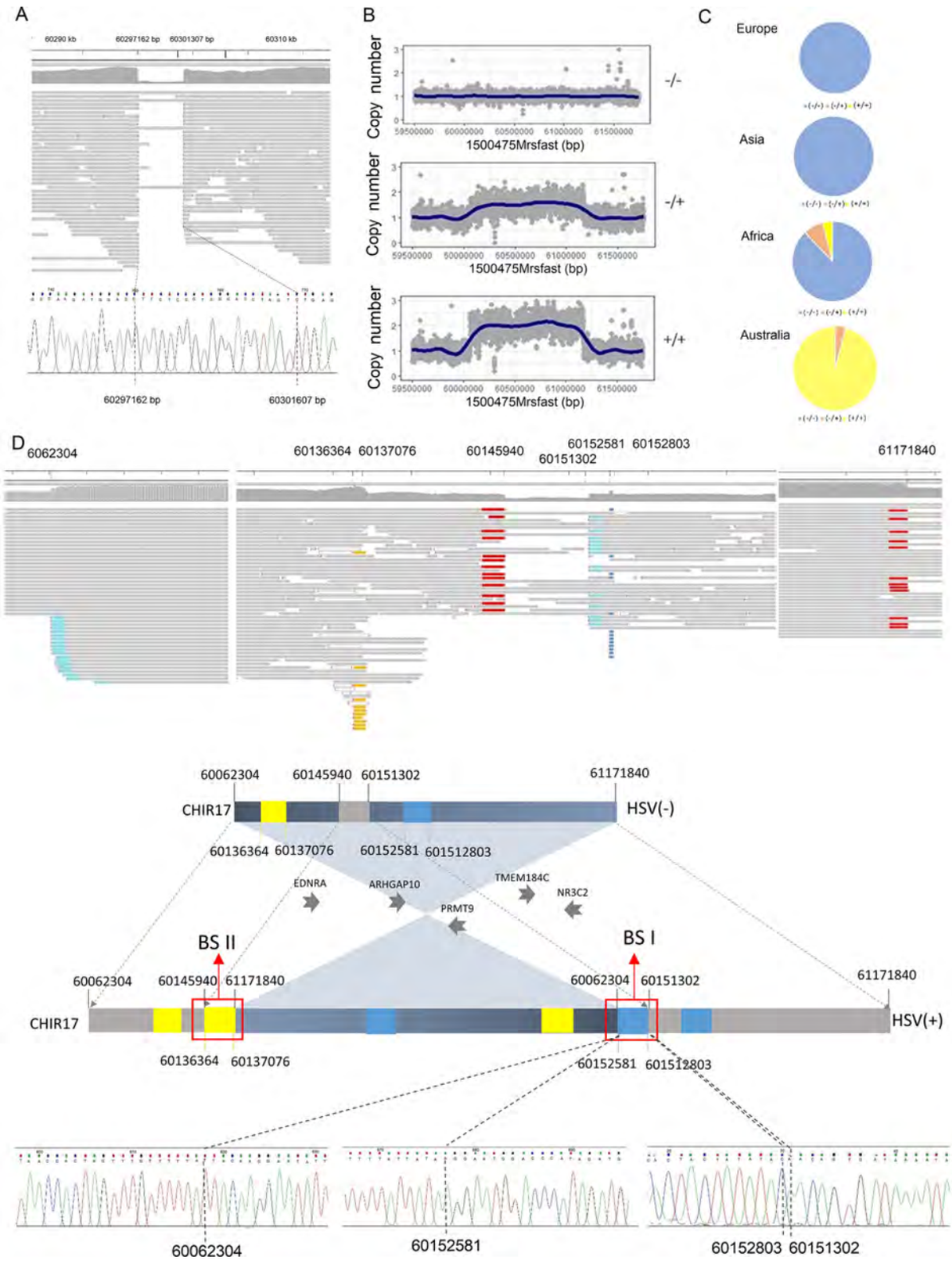

Figure 2 Genomic structure of HSV on CHIR17 in goats

A: IGV screenshots of Nanopore long-read sequences, showing lack of the 4 145 bp spacer sequence between CNV1 and CNV2, as determined by long-read and PCR-Sanger sequencing of homozygous goats. B: Coverage of genomic reads of different genotypes of HSV. C: Genotype frequency distribution of homozygous duplicated HSV (+/+) in different geographical populations. D: Close-ups of IGV screenshots of Illumina long-read sequences, illustrating duplication of CHIR17 at the boundaries of the variant sites. Red and green reads are mapped at different locations. Extremely prominent multicopy elements (MCE1, MCE2) are in yellow and blue. E: Schematic of variant on CHIR17, showing inversely inserted ~1.1 Mb segment and deleted 5 363 bp region (CHIR17:60145940–60151302 bp) by retrovirus direction; location and orientation of annotated genes and loci in involved genome regions are shown. F: Experimental confirmation of complex structural variant. Sanger sequencing of PCR products of variant allele precisely defines breakpoints of fusion of CHIR17 segments.

directions (Figure 2D). Therefore, we initially assumed that the chromosomal rearrangement structure of the HSV was formed by the insertion of the extra 1.11 Mb duplication in the reverse orientation and by the deletion of the ~5.3 kb region (Figure 2E). Here, the two end sequences of the HSV reverse insertion sites were named boundary sequence I (BS I, CHIR17: 60062304 bp) and boundary sequence II (BS II, CHIR17:61171840 bp). We designed primers extending approximately 1 kb on each side of BS I, which were then verified by PCR-Sanger sequencing. The product sequence results are shown in Figure 2F. The primers designed at each 1 kb extension of BS II and PCR amplification were unsuccessful and accurate sequence assignments were not obtained due to deficiencies in the reference genome assembly.

Two extremely prominent multicopy elements (MCEs) were widely observed in the HSV region (Figure 2D), including MCE1 (718 bp in size, mapped to CHIR17:60136360–60137078 bp) and MCE2 (222 bp in size, mapped to CHIR17:60152581–60152803 bp). Some duplicate reads of both elements were also positioned adjacent to BS I (Supplementary Figure S1) and BS II (Supplementary Figure S2). Although a nucleic acid BLAST search of the NCBI database did not retrieve any information on MCE2, MCE1 showed 96.6% similarity to *Babesia ovata* Retrovirus-related Pol poly LINE-1 (XM_029013938.1).

Cell culture, identification, and transfection

According to the KEGG results of the five genes within the 1.11 Mb duplicated region, only three were enriched in KEGG pathways related to bacterial invasion of epithelial cells (*ARHGAP10*), vascular smooth muscle contraction (*EDNRA*), and aldosterone-regulated sodium reabsorption (*NR3C2*).

The isolated and cultured SMSCs were identified by immunofluorescence (Wang et al., 2020). Results showed that the expression efficiency of Pax7 was 82.3% (Supplementary Figure S3A). Infection efficiency was assessed using different multiplicities of infection (MOIs: 30, 60, 90, and 120) (Supplementary Figure S4). At an MOI of 90, the fluorescence intensity was highest and SMSCs grew well (Supplementary Figure S3B). At 48 h after lentiviral transfection, the gene expression levels of *ARHGAP10*, *NR3C2*, and *EDNRA* were significantly higher than those in the control group (P<0.01; Supplementary Figure S3C).

Involvement of overexpressed candidate genes (*ARHGAP10*, *NR3C2*, and *EDNRA*) in proliferation and differentiation of SMSCs

The effects of the three candidate genes on SMSC proliferation were determined by the CCK-8 method. Cells proliferated rapidly within 24–36 h after lentiviral transfection, and the proliferation rate of SMSCs transfected with *ARHGAP10* and *NR3C2* overexpressing lentiviruses was significantly higher than that of the control cells (Figure 3C). We also examined the proliferation of SMSCs by EdU assay and found that *ARHGAP10* and *NR3C2* overexpression significantly increased the number of EdU-positive cells in the proliferation phase (Figure 3A, B).

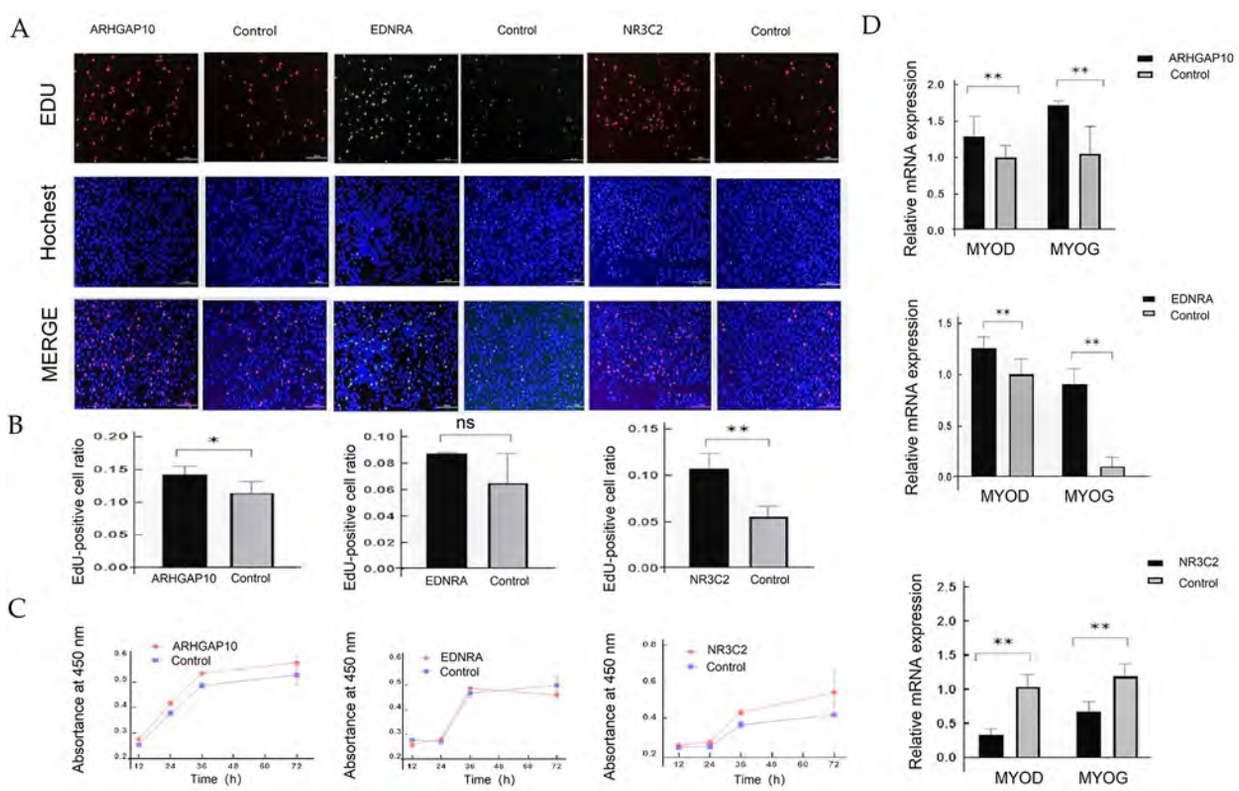

Figure 3 Effects of overexpression of *ARHGAP10*, *NR3C2*, and *EDNRA* or control on SMSC proliferation and differentiation

A: EdU assay results for SMSCs after overexpression of *ARHGAP10*, *NR3C2*, and *EDNRA* for 48 h, where EdU (red) fluorescence indicates proliferation and Hoechst (blue) fluorescence indicates nuclei. B: EdU-positive cell ratio of SMSCs after overexpression of *ARHGAP10*, *NR3C2*, and *EDNRA* for 48 h. Data are mean±standard error of the mean (*SEM*) (n=6). C: Cell growth curves of SMSCs measured by CCK-8 Kit after overexpression. D: Effects of mRNA expression of *MyHC*, *MyoD*, and *MyoG* in overexpressed *ARHGAP10*, *NR3C2*, and *EDNRA* genes on SMSC differentiation. ns: No significance; *: P<0.05; **: P<0.01 vs. Control.

The differentiation effects observed after SMSCs were induced to differentiate for 4 days is shown in Supplementary Figure S5. Analysis of the effects of candidate gene overexpression on SMSC differentiation revealed that the relative mRNA expression levels of differentiation marker genes (*MyoD* and *MyoG*) increased after transfection with *ARHGAP10*- and *EDNRA*-carrying lentiviruses (Figure 3D). In contrast, the relative mRNA expression levels of *MyoD* and *MyoG* were inhibited in SMSCs after *NR3C2* transfection.

Molecular heredity regulation basis of overexpressed candidate genes in SMSCs

To further understand the regulatory mechanism of the *ARHGAP10*, *NR3C2*, and *EDNRA* genes in goat SMSCs, we performed RNA-seq of the transfected SMSCs and identified changes in related genes during cell proliferation and differentiation. A total of 273 significant DEGs were identified in the NA versus NO group, including 228 up-regulated genes (e.g., *BMP2*, *MYH3*, and *MYORG*) and 45 down-regulated genes (e.g., *EGR3*, *HAS2*, and *LIF*) (Figure 4A). Five significant DEGs (*CFB*, *C2*, *CYP26B1*, *SLC7A8*, and *SLPI*) were identified in the EA versus EO group, all of which were significantly up-regulated. One significant DEG (*SAA3*) was identified in the AA versus AO group, which was significantly up-regulated.

In the NA versus NO group, 125 DEGs were enriched in 223 pathways (Figure 4B), including several well-known pathways involved in cell growth and muscle development, such as the calcium signaling pathway, cyclic guanosine monophosphate-dependent protein kinase G (cGMP-PKG) signaling pathway, and transforming growth factor (TGF) signaling pathway. Many DEGs (e.g., *TGF-B2*, *MYH3*, *ANKRD1*, and *MYH15*) were involved in growth and development (Figure 4C), including muscle cell differentiation (e.g., muscle cell differentiation and cardiac muscle cell cycle based on GO annotation).

We also explored mRNA expression of DEGs in the NA versus NO group (Figure 5A) and EA versus EO group (Figure 5B). Notably, mRNA expression of *SAA3* was up-regulated in the SMSCs after overexpression of *ARHGAP10*, *EDNRA*, and *NR3C2* (Figure 5C). DEG validation by qRT-PCR was consistent with the RNA-seq results, confirming the stability and reliability of the transcriptome data in this study.

DISCUSSION

In this study, Australian Boer goats were shown to carry a high frequency of a homozygous-duplicated genotype of HSV. This duplicated genotype was not found in indigenous European and Asian goats but was detected at a low frequency in indigenous African goats. This finding suggests that this duplicated genotype may have originated from Africa, as Boer goats were initially bred by crossing indigenous African goats with European goats (Malan, 2000).

A large number of chromosomal rearrangements are distributed within vertebrate genomes (Tsai & Lieber, 2010), which are involved in a wide variety of biological functions and the formation of various phenotypes (Castronovo et al., 2015; Kot et al., 2021). A potential lentiviral transposable sequence appeared at junctional boundaries formed by the HSV chromosomal rearrangements. Various studies have shown that repetitive sequence elements of retroviruses may lead to large-scale chromosomal deletions, duplications, and rearrangements via homologous recombination (Hughes & Coffin, 2001). Evidence suggests that the frequency of rearrangements is higher when the LINE-1 copy number within the genomic region is high (Kemp & Longworth, 2015). Hence, HSV may be a retrovirus-directed chromosomal rearrangement.

Several studies have demonstrated that CNVs can promote phenotypic variation through dosage effects on gene expression (Berkel & Cacan, 2022; Pielberg et al., 2003). Evidence also suggests that the three genes within HSV identified in our study are involved in the development of

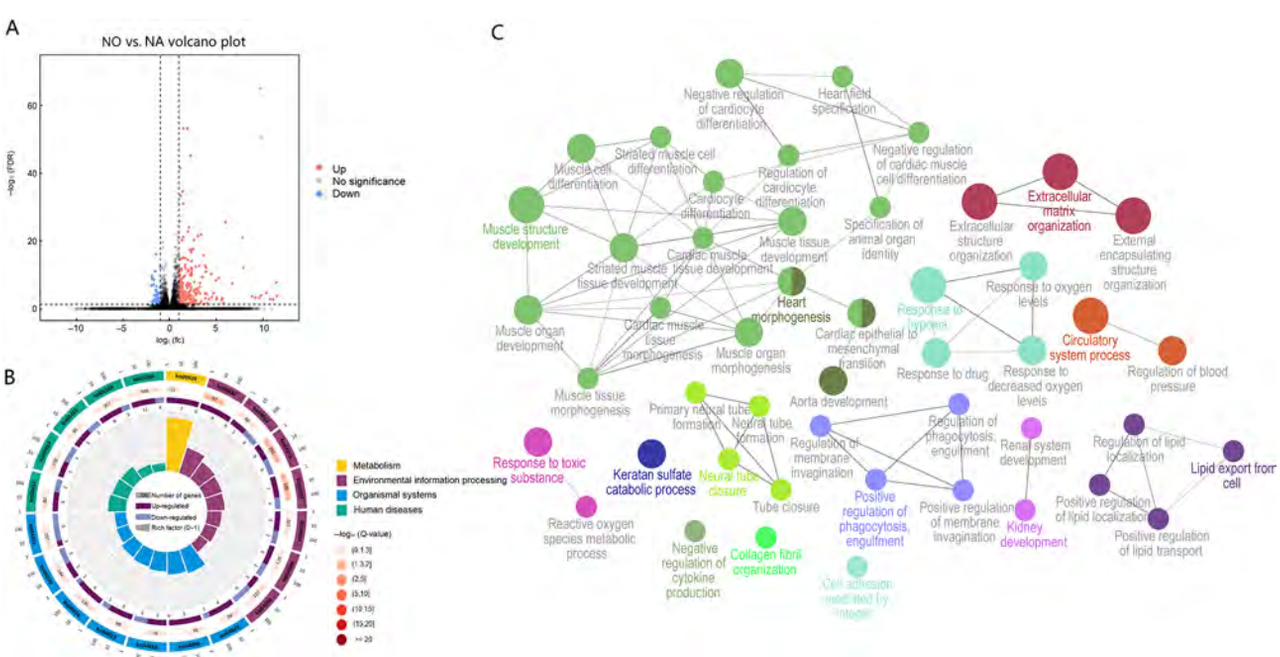

Figure 4 Transcriptomic changes in SMSCs after *NR3C2* overexpression

A: Volcano plot clustering of DEGs in samples transfected with overexpressed *NR3C2*. B: Pathways of DEGs in NA versus NO group according to KEGG enrichment analysis. C: Network diagram of GO terms enriched in DEGs in NA vs. NO group.

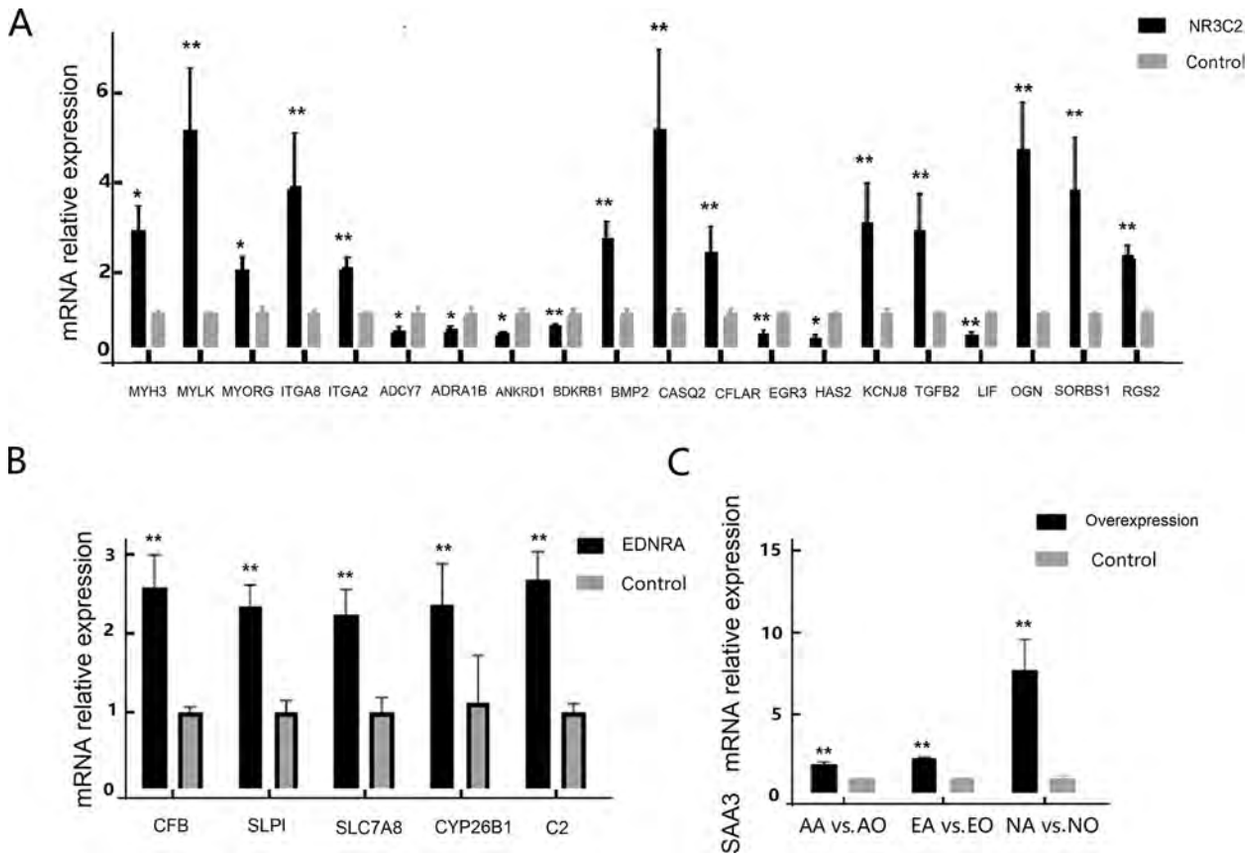

Figure 5 Results of mRNA expression of DEGs

A: mRNA expression of DEGs involved in muscle development in samples transfected with overexpressed *NR3C2* or control. B: mRNA expression of DEGs in samples transfected with overexpressed *EDNRA* or control. C: mRNA expression of *SAA3* in SMSCs after overexpression of *ARHGAP10*, *EDNRA*, and *NR3C2*. Data are mean±*SEM* (*n*=6). *: *P*<0.05; **: *P*<0.01 vs. control.

muscle cells. For example, Rho GTPase activating protein 10 (*ARHGAP10*) not only regulates the Rho-GTPase signaling pathway associated with actin cytoskeleton dynamics and cell proliferation and differentiation by encoding a potential cytoskeletal Rho-GTPase-activating protein but is also highly expressed in muscles and involved in cell differentiation (Bassères et al., 2002; Shibata et al., 2001). Coincidentally, *ARHGAP10* is reported to be involved in the formation of intramuscular fat in Japanese black cattle (Ueda et al., 2021). Nuclear receptor subfamily 3 group C member 2 (*NR3C2*) is a key component of hypothalamic-pituitary-adrenal neuroendocrine axis regulation, and variants in this gene are associated with muscle glycogen content and meat quality traits in male Nellore cattle (Poleti et al., 2015). *NR3C2* also contributes to muscular dystrophy relief and skeletal muscle repair in acute muscle injury (Howard et al., 2022). Endothelin receptor type A (*EDNRA*) is involved in various physiological functions, including smooth muscle contraction and fetal muscle development (Kobayashi et al., 2016; Sato et al., 2008).

The development of skeletal muscles is determined by the co-regulation of multiple signaling pathways, such as the adherens junction and Ca^{+} signaling pathways (Su et al., 2018). In addition, mTOR plays an essential role in satellite cell function and skeletal muscle regeneration by controlling the expression of myogenic genes (Zhang et al., 2015), while WNT is involved in myogenesis, neuromuscular synapses, and fibrosis (Cisternas et al., 2014). Specifically, activation of the TNF, MAPK/ERK, and PI3K/Akt pathways promotes proliferation and differentiation of adult muscle cells (Elia et al., 2007). Furthermore, the DNA methylation status of Wnt and TGF-β signaling is a key factor regulating SMSC development and function (Zhang et al., 2019). Here, many of the above-mentioned pathways were enriched in DEGs according to the NA versus NO RNA-seq results, indicating that *NR3C2* is involved in the signal transduction of many regulatory pathways related to skeletal muscle development.

Muscle satellite cells play a critical role in muscle growth via activation of the cell cycle in quiescent satellite cells (Chang & Rudnicki, 2014). Based on GO analysis, many DEGs from the NA versus NO RNA-seq group were associated with the cell cycle. For example, up-regulation of interferon regulatory factor 1 (*IRF1*) can accelerate cell cycle progression (Zhang et al., 2013), and growth arrest and DNA damage-inducible gene gamma (*GADD45G*) is associated with cell cycle checkpoints, apoptosis, and DNA repair (Humayun & Fornace, 2022). The centrosome scaffold protein (CEP192) recruits mitotic protein kinases Aurora A and PLK1 to the centrosome, and is essential for bipolar spindle assembly with centrioles to promote bipolar spindle formation and cell cycle regulation (Chinen et al., 2021; Nasa et al., 2017). Up-regulation of the adenosine triphosphate-binding cassette subfamily B member 1 (*ABCB1*) can reduce cell viability, promote apoptosis, and induce cell cycle arrest in G2/M (Zhou et al., 2019).

Satellite cell activation is accompanied by extensive cell migration (Yin et al., 2013). Our GO analysis results confirmed that DEGs from the NA versus NO RNA-seq group were involved in cell migration and positive regulation. For example,

as an important cytoskeletal protein, NEDD9 regulates cell proliferation, migration, invasion, and survival (Wang et al., 2017a). Bradykinin receptor B1 (*BDKRB1*) is a specific regulator of immune cell entry into the central nervous system and regulates lymphocyte migration across the blood-brain barrier endothelium *in vitro* (Schulze-Topphoff et al., 2009). Bradykinin expression can also induce the migration and invasion of glioma cells through *BDKRB1*-mediated calcium influx and subsequent behavior (Sun et al., 2020).

Complete skeletal muscle growth and repair includes SMSC growth and proliferation, myotube fusion, and myoblast production (Delaney et al., 2017). Here, many DEGs identified in the NA versus NO RNA-seq group were involved in these biological processes. In particular, functional loosening of cadherin 1 (*CDH1*) can promote and prevent quiescent SMSCs from switching on the cell cycle and ultimately compensates for the proliferation of muscle precursor cells (Christensen et al., 2007). Overexpression of CASP8 and FADD-like apoptosis regulator (*CFLAR*), also known as *c-FLIP*, can induce nuclear factor-κB (NF-κB) activation and promote SMSC proliferation (Giampietri et al., 2010). Early growth response 3 (*EGR3*), a zinc finger transcription factor, regulates diverse cellular functions and is involved in muscle cell proliferation (Kurosaka et al., 2017). Reduced *EGR3* expression is associated with attenuated function of SMSCs and hinders muscle cell regeneration in aged individuals (Ogura et al., 2020). Ankyrin repeat domain protein 1 (ANKRD1) is a transcriptional co-regulator in striated muscles and is involved in myofibril assembly (Boskovic et al., 2018). Skeletal muscle regeneration is also controlled by various extracellular factors, such as *TGF-β2*, which encodes transforming growth factor β2; this protein regulates skeletal muscle growth, stimulates SMSC proliferation, and restores muscle regeneration potential by perturbing β-catenin in SMSCs (Rudolf et al., 2016). In addition, fatty acid translocase cluster of differentiation (*CD36*) is not only related to the binding and transport of long-chain fatty acids but is also involved in fatty acid metabolism in skeletal muscles (Ibrahimi et al., 1999). Studies have reported that *CD36* deficiency impairs SMSC function and delays muscle regeneration (Verpoorten et al., 2020).

Six DEGs were identified in the EA versus EO RNA-seq group, which are widely involved in biological processes, such as growth and immunity. Cytochrome P450 family 26 subfamily B member 1 (*CYP26B1*) can regulate tongue muscle differentiation via retinoic acid signaling (Okano et al., 2008). *CYP26B1* also promotes maxillary tendon condensation and musculoskeletal patterning in zebrafish embryos (McGurk et al., 2017). Complement factor B (*CFB*) is involved in an alternative pathway of complement expression in muscle cells *in vitro*, with evidence showing that local complement expression in skeletal muscles is associated with certain muscle inflammatory or pathological processes *in vivo* (Legoedec et al., 1995). *SLC7A8* expression impairs proteolysis and affects carcass characteristics and meat quality in yak (Liu et al., 2021). Finally, secretory leukoprotease inhibitor (*SLPI*) can suppress proinflammatory cytokine production in lipopolysaccharide-stimulated cells, prevent neutrophil infiltration in mouse models of lung and liver injury, and modulate activity of transcription factor NF-κB (Douglas & Hannila, 2022).

This study showed that overexpression of all candidate genes significantly up-regulated the transcriptional expression of serum amyloid antigen 3 (*SAA3*). Abnormal local inflammatory signaling of skeletal muscles is considered a contributing factor in sarcopenia (Buford et al., 2009). The *SAA* family, consisting of major vertebrate acute-phase reactants, plays an important role in host defense during inflammation (Uhlar & Whitehead, 1999). *SAA3* is associated with obesity and insulin resistance in humans (Scheja et al., 2008). Specifically, *SAA3* levels show a positive correlation with obesity (Ji et al., 2022). Furthermore, *Lycium barbarum* polysaccharide can improve diabetes by inhibiting the effects of NF-κB activation in mouse models of diabetic nephropathy to reduce *SAA3* expression (Wan et al., 2022). In addition, studies have reported that *SAA3* is required for normal weight and immunometabolic function of *SLC2A3* in mice (Ather & Poynter, 2018).

CONCLUSIONS

The proliferation and differentiation of SMSCs play an important role in muscle development. Our study first identified the complex structure of a high frequency 1.1 Mb duplication CNV in Boer goats and clarified that a dosage effect on the expression of overlapping genes (*ARHGAP10*, *NR3C2*, and *EDNRA*) significantly contributed to SMSC proliferation and differentiation. This study not only improves our understanding of the genetic basis for the excellent growth performance of Boer goats but also provides new insights into the molecular regulation of muscle development.

DATA AVAILABILITY

All data in this article can be downloaded from the NCBI (PRJNA843937), GSA (PRJCA013855), and Science Data Bank databases (DOI:10.57760/sciencedb.j00139.00043).

SUPPLEMENTARY DATA

Supplementary data to this article can be found online.

COMPETING INTERESTS

The authors declare that they have no competing interests.

AUTHORS' CONTRIBUTIONS

Y.Y., W.Y.Z., and G.X.E. designed the project. B.G.Y., D.K.Z., L.X., and Y.M.H. contributed to blood sample collection. H.Y.Z. and L.C.L. analyzed the data. B.O., Y.G.H., Y.Z., K.K., M.X.C., H.Z.J., H.P.Z., and Y.W.S. contributed to data collection for experimental validation. Y.Y. and G.X. E. wrote the paper. Y.H.M., W.G.Z., H.J.G., L.J., F.P.Z., L.P.Z., R.S.N., S.Z.W., X.P.J., J.L.H., H.L., Y.F.H., Y.J.Z., and Z.Q.Z. reviewed and edited the manuscript. All authors read and approved the final version of the manuscript.

ACKNOWLEDGEMENTS

The authors thank Dr. Zhu-Qing Zheng for help in software analysis.

REFERENCES

Adewoye AB, Shrine N, Odenthal-Hesse L, et al. 2018. Human *CCL3L1* copy number variation, gene expression, and the role of the CCL3L1-CCR5 axis in lung function. *Wellcome Open Research*, **3**: 13.

Ather JL, Poynter ME. 2018. Serum amyloid A3 is required for normal weight and immunometabolic function in mice. *PLoS One*, **13**(2): e0192352.

Bassères DS, Tizzei EV, Duarte AAS, et al. 2002. ARHGAP10, a novel human gene coding for a potentially cytoskeletal Rho-GTPase activating protein. *Biochemical and Biophysical Research Communications*, **294**(3): 579−585.

Berkel C, Cacan E. 2022. Copy number and expression of CEP89, a protein

required for ciliogenesis, are increased and predict poor prognosis in patients with ovarian cancer. *Cell Biochemistry & Function*, **40**(3): 298−309.
Bezerra H, Santos E, Oliveira J, et al. 2019. Performance and ruminal parameters of boer crossbred goats fed diets that contain crude glycerin. *Animals*, **9**(11): 967.
Bi Y, He LB, Feng B, et al. 2021. A 5-bp mutation within *MSTN/GDF8* gene was significantly associated with growth traits in Inner Mongolia White Cashmere goats. *Animal Biotechnology*, **32**(5): 610−615.
Boskovic S, Marín-Juez R, Jasnic J, et al. 2018. Characterization of zebrafish (*Danio rerio*) muscle ankyrin repeat proteins reveals their conserved response to endurance exercise. *PLoS One*, **13**(9): e0204312.
Buford TW, Cooke MB, Willoughby DS. 2009. Resistance exercise-induced changes of inflammatory gene expression within human skeletal muscle. *European Journal of Applied Physiology*, **107**(4): 463−471.
Castronovo C, Crippa M, Bestetti I, et al. 2015. Complex *de novo* chromosomal rearrangement at 15q11-q13 involving an intrachromosomal triplication in a patient with a severe neuropsychological phenotype: clinical report and review of the literature. *Amercian Journal of Medical Genetics Part A*, **167**(1): 221−230.
Chang NC, Rudnicki MA. 2014. Satellite cells: the architects of skeletal muscle. *Current Topics in Developmental Biology*, **107**: 161−181.
Chaosap C, Sitthigripong R, Sivapirunthep P, et al. 2020. Myosin heavy chain isoforms expression, calpain system and quality characteristics of different muscles in goats. *Food Chemistry*, **321**: 126677.
Chinen T, Yamazaki K, Hashimoto K, et al. 2021. Centriole and PCM cooperatively recruit CEP192 to spindle poles to promote bipolar spindle assembly. *Journal of Cell Biology*, **220**(2): e202006085.
Christensen KL, Brennan JDG, Aldridge CS, et al. 2007. Cell cycle regulation of the human Six1 homeoprotein is mediated by APC^{Cdh1}. *Oncogene*, **26**(23): 3406−3414.
Cisternas P, Henriquez JP, Brandan E, et al. 2014. Wnt signaling in skeletal muscle dynamics: myogenesis, neuromuscular synapse and fibrosis. *Molecular Neurobiology*, **49**(1): 574−589.
Delaney K, Kasprzycka P, Ciemerych MA, et al. 2017. The role of TGF-β1 during skeletal muscle regeneration. *Cell Biology International*, **41**(7): 706−715.
Dodson MV, Hausman GJ, Guan LL, et al. 2010. Skeletal muscle stem cells from animals I. Basic cell biology. *International Journal of Biological Sciences*, **6**(5): 465−474.
Douglas TC, Hannila SS. 2022. Working from within: how secretory leukocyte protease inhibitor regulates the expression of pro-inflammatory genes. *Biochemistry and Cell Biology*, **100**(1): 1−8.
Dumont NA, Bentzinger CF, Sincennes MC, et al. 2015. Satellite cells and skeletal muscle regeneration. *Comprehensive Physiology*, **5**(3): 1027−1059.
Elia D, Madhala D, Ardon E, et al. 2007. Sonic hedgehog promotes proliferation and differentiation of adult muscle cells: involvement of MAPK/ERK and PI3K/Akt pathways. *Biochimica et Biophysica Acta* (*BBA*)-*Molecular Cell Research*, **1773**(9): 1438–1446.
Feng XS, Naz F, Juan AH, et al. 2018. Identification of skeletal muscle satellite cells by immunofluorescence with Pax7 and laminin antibodies. *Journal of Visualized Experiments:JoVE*, (134): 57212.
Giampietri C, Petrungaro S, Coluccia P, et al. 2010. c-Flip overexpression affects satellite cell proliferation and promotes skeletal muscle aging. *Cell Death & Disease*, **1**(4): e38.
Giordani L, Parisi A, Le Grand F. 2018. Satellite cell self-renewal. *Current Topics in Developmental Biology*, **126**: 177−203.
Howard ZM, Rastogi N, Lowe J, et al. 2022. Myeloid mineralocorticoid receptors contribute to skeletal muscle repair in muscular dystrophy and acute muscle injury. *American Journal of Physiology-Cell Physiology*, **322**(3): C354−C369.
Huang YZ, Li YJ, Wang XH, et al. 2021. An atlas of CNV maps in cattle, goat and sheep. *Science China Life Sciences*, **64**(10): 1747−1764.
Hughes JF, Coffin JM. 2001. Evidence for genomic rearrangements mediated by human endogenous retroviruses during primate evolution. *Nature Genetics*, **29**(4): 487−489.
Humayun A, Fornace AJ Jr. 2022. GADD45 in stress signaling, cell cycle control, and apoptosis. *In*: Zaidi MR, Liebermann DA. Gadd45 Stress Sensor Genes. Cham: Springer, 1–22.
Ibrahimi A, Bonen A, Blinn WD, et al. 1999. Muscle-specific overexpression of FAT/CD36 enhances fatty acid oxidation by contracting muscle, reduces plasma triglycerides and fatty acids, and increases plasma glucose and insulin. *Journal of Biological Chemistry*, **274**(38): 26761−26766.
Ji A, Trumbauer AC, Noffsinger VP, et al. 2022. Serum Amyloid A is not obligatory for high-fat, high-sucrose, cholesterol-fed diet-induced obesity and its metabolic and inflammatory complications. *PLoS One*, **17**(4): e0266688.
Kemp JR, Longworth MS. 2015. Crossing the LINE toward genomic instability: LINE-1 retrotransposition in cancer. *Frontiers in Chemistry*, **3**: 68.
Kholif AE, Hamdon HA, Kassab AY, et al. 2020. *Chlorella vulgaris* microalgae and/or copper supplementation enhanced feed intake, nutrient digestibility, ruminal fermentation, blood metabolites and lactational performance of Boer goat. *Journal of Animal Physiology and Animal Nutrition*, **104**(6): 1595−1605.
Kobayashi Y, Yoshimoto Y, Yamamoto Y, et al. 2016. Roles of EDNs in regulating oviductal NO synthesis and smooth muscle motility in cows. *Reproduction*, **151**(6): 615−622.
Kot P, Yasuhara T, Shibata A, et al. 2021. Mechanism of chromosome rearrangement arising from single-strand breaks. *Biochemical and Biophysical Research Communications*, **572**: 191−196.
Kurosaka M, Ogura Y, Funabashi T, et al. 2017. Early growth response 3 (Egr3) contributes a maintenance of C2C12 myoblast proliferation. *Journal of Cellular Physiology*, **232**(5): 1114−1122.
Ladeira GC, Pilonetto F, Fernandes AC, et al. 2022. CNV detection and their association with growth, efficiency and carcass traits in Santa Inês sheep. *Journal of Animal Breeding and Genetics*, **139**(4): 476−487.
Legoedec J, Gasque P, Jeanne JF, et al. 1995. Expression of the complement alternative pathway by human myoblasts *in vitro*: biosynthesis of C3, factor B, factor H and factor I. *European Journal of Immunology*, **25**(12): 3460−3466.
Li B, Dewey CN. 2011. RSEM: accurate transcript quantification from RNA-Seq data with or without a reference genome. *BMC Bioinformatics*, **12**: 323.
Liu M, Zhou Y, Rosen BD, et al. 2019. Diversity of copy number variation in the worldwide goat population. *Heredity*, **122**(5): 636−646.
Liu YX, Ma XM, Xiong L, et al. 2021. Effects of intensive fattening with total mixed rations on carcass characteristics, meat quality, and meat chemical composition of yak and mechanism based on serum and transcriptomic profiles. *Frontiers in Veterinary Science*, **7**: 599418.
Livak KJ, Schmittgen TD. 2001. Analysis of relative gene expression data using real-time quantitative PCR and the 2(-Delta Delta C(T)) Method. *Methods*, **25**(4): 402−408.
Love MI, Huber W, Anders S. 2014. Moderated estimation of fold change and dispersion for RNA-seq data with DESeq2. *Genome Biology*, **15**(12): 550.
Lye ZN, Purugganan MD. 2019. Copy number variation in domestication. *Trends in Plant Science*, **24**(4): 352−365.
Malan SW. 2000. The improved Boer goat. *Small Ruminant Research*, **36**(2): 165−170.
Marques JI, Leite PG, Lopes Neto JP, et al. 2021. Estimation of heat exchanges in Boer crossbred goats maintained in a climate chamber. *Journal of Thermal Biology*, **96**: 102832.
McGurk PD, Swartz ME, Chen JW, et al. 2017. *In vivo* zebrafish morphogenesis shows Cyp26b1 promotes tendon condensation and

musculoskeletal patterning in the embryonic jaw. *PLoS Genetics*, **13**(12): e1007112.

Metzger K, Tuchscherer A, Palin MF, et al. 2020. Establishment and validation of cell pools using primary muscle cells derived from satellite cells of pig skeletal muscle. *In Vitro Cellular & Developmental Biology. Animal*, **56**(3): 193−199.

Milewska M, Grabiec K, Grzelkowska-Kowalczyk K. 2014. Interactions of proliferation and differentiation signaling pathways in myogenesis. *Postepy Higieny I Medycyny Doswiadczalnej* (*Online*), **68**: 516–526.

Nasa I, Trinkle-Mulcahy L, Douglas P, et al. 2017. Recruitment of PP1 to the centrosomal scaffold protein CEP192. *Biochemical and Biophysical Research Communications*, **484**(4): 864−870.

Ncube KT, Dzomba EF, Hadebe K, et al. 2022. Carcass quality profiles and associated genomic regions of south african goat populations investigated using goat SNP50K genotypes. *Animals* (*Basel*), **12**(3): 364.

Ogura Y, Sato S, Kurosaka M, et al. 2020. Age-related decrease in muscle satellite cells is accompanied with diminished expression of early growth response 3 in mice. *Molecular Biology Reports*, **47**(2): 977−986.

Okano J, Sakai Y, Shiota K. 2008. Retinoic acid down-regulates *Tbx1* expression and induces abnormal differentiation of tongue muscles in fetal mice. *Developmental Dynamics*, **237**(10): 3059−3070.

Paudel Y, Madsen O, Megens HJ, et al. 2013. Evolutionary dynamics of copy number variation in pig genomes in the context of adaptation and domestication. *BMC Genomics*, **14**: 449.

Pérez-Baena I, Jarque-Durán M, Gómez EA, et al. 2021. Terminal crossbreeding of murciano-granadina goats to boer bucks: effects on reproductive performance of goats and growth of kids in artificial rearing. *Animals* (*Basel*), **11**(4): 986.

Pielberg G, Day AE, Plastow GS, et al. 2003. A sensitive method for detecting variation in copy numbers of duplicated genes. *Genome Research*, **13**(9): 2171−2177.

Poleti MD, DeRijk RH, Rosa AF, et al. 2015. Genetic variants in glucocorticoid and mineralocorticoid receptors are associated with concentrations of plasma cortisol, muscle glycogen content, and meat quality traits in male Nellore cattle. *Domestic Animal Endocrinology*, **51**: 105−113.

Relaix F, Zammit PS. 2012. Satellite cells are essential for skeletal muscle regeneration: the cell on the edge returns centre stage. *Development*, **139**(16): 2845−2856.

Rudolf A, Schirwis E, Giordani L, et al. 2016. β-Catenin activation in muscle progenitor cells regulates tissue repair. *Cell Reports*, **15**(6): 1277−1290.

Sato T, Kawamura Y, Asai R, et al. 2008. Recombinase-mediated cassette exchange reveals the selective use of G_q/G_{11}-dependent and -independent endothelin 1/endothelin type A receptor signaling in pharyngeal arch development. *Development*, **135**(4): 755−765.

Scheja L, Heese B, Zitzer H, et al. 2008. Acute-phase serum amyloid A as a marker of insulin resistance in mice. *Journal of Diabetes Research*, **2008**: 230837.

Schulze-Topphoff U, Prat A, Prozorovski T, et al. 2009. Activation of kinin receptor B1 limits encephalitogenic T lymphocyte recruitment to the central nervous system. *Nature Medicine*, **15**(7): 788−793.

Shakweer WMES, El-Rahman HHA. 2020. Cloning, nucleotide sequencing, and bioinformatics analyses of growth hormone mRNA of Assaf sheep and Boer goats reared in Egypt. *Journal of Genetic Engineering and Biotechnology*, **18**(1): 30.

Shao X, Lv N, Liao J, et al. 2019. Copy number variation is highly correlated with differential gene expression: a pan-cancer study. *BMC Medical Genetics*, **20**(1): 175.

Shen Y, Yan YL, Liu YQ, et al. 2013. A significant effect of the *TSPY1* copy number on spermatogenesis efficiency and the phenotypic expression of the gr/gr deletion. *Human Molecular Genetics*, **22**(8): 1679−1695.

Shibata H, Oishi K, Yamagiwa A, et al. 2001. PKNβ interacts with the SH3 domains of Graf and a novel Graf related protein, Graf 2, which are GTPase activating proteins for Rho family. *The Journal of Cellular Biochemistry*, **130**(1): 23−31.

Shishido E, Aleksic B, Ozaki N. 2014. Copy-number variation in the pathogenesis of autism spectrum disorder. *Psychiatry and Clinical Neurosciences*, **68**(2): 85−95.

Su XT, Zhao YF, Wang YN, et al. 2018. Overexpression of the *Rybp* gene inhibits differentiation of bovine myoblasts into myotubes. *International Journal of Molecular Sciences*, **19**(7): 2082.

Sun DP, Lee YW, Chen JT, et al. 2020. The bradykinin-BDKRB1 axis regulates *Aquaporin 4* gene expression and consequential migration and invasion of malignant glioblastoma cells via a Ca^{2+}-MEK1-ERK1/2-NF-κB mechanism. *Cancers* (*Basel*), **12**(3): 667.

Tsai AG, Lieber MR. 2010. Mechanisms of chromosomal rearrangement in the human genome. *BMC Genomics*, **11 Suppl 1**(Suppl 1): S1.

Ueda S, Hosoda M, Yoshino KI, et al. 2021. Gene expression analysis provides new insights into the mechanism of intramuscular fat formation in japanese black cattle. *Genes* (*Basel*), **12**(8): 1107.

Uhlar CM, Whitehead AS. 1999. Serum amyloid A, the major vertebrate acute-phase reactant. *European Journal of Biochemistry*, **265**(2): 501−523.

van Wyk GL, Hoffman LC, Strydom PE, et al. 2022. Differences in meat quality of six muscles obtained from southern african large-frame indigenous veld goat and boer goat wethers and bucks. *Animals* (*Basel*), **12**(3): 382.

Veal CD, Reekie KE, Lorentzen JC, et al. 2014. A 129-kb deletion on chromosome 12 confers substantial protection against rheumatoid arthritis, implicating the gene *SLC2A3*. *Human Mutation*, **35**(2): 248–256.

Verpoorten S, Sfyri P, Scully D, et al. 2020. Loss of CD36 protects against diet-induced obesity but results in impaired muscle stem cell function, delayed muscle regeneration and hepatic steatosis. *Acta Physiologica*, **228**(3): e13395.

Wan FQ, Ma FL, Wu JX, et al. 2022. Effect of *Lycium barbarum* polysaccharide on decreasing serum amyloid A3 expression through inhibiting NF-κB activation in a mouse model of diabetic nephropathy. *Analytical Cellular Pathology*, **2022**: 7847135.

Wang J, Wang S, Luan Y, et al. 2017a. Overexpression of NEDD9 in renal cell carcinoma is associated with tumor migration and invasion. *Oncology Letters*, **14**(6): 8021−8027.

Wang LJ, Zhu YH, Liu X, et al. 2019a. Glycogen synthase kinase 3β (GSK3β) regulates the expression of MyHC2a in goat skeletal muscle satellite cells (SMSCs). *Animal Science Journal*, **90**(8): 1042−1049.

Wang WT, Sun B, Hu P, et al. 2019b. Comparison of differential flavor metabolites in meat of lubei white goat, Jining gray goat and boer goat. *Metabolites*, **9**(9): 176.

Wang XH, Zheng ZQ, Cai YD, et al. 2017b. CNVcaller: highly efficient and widely applicable software for detecting copy number variations in large populations. *Gigascience*, **6**(12): 1−12.

Wang Y, Xiao X, Wang LJ. 2020. *In vitro* characterization of goat skeletal muscle satellite cells. *Animal Biotechnology*, **31**(2): 115−121.

Wu HQ, Ren Y, Pan W, et al. 2015. The mammalian target of rapamycin signaling pathway regulates myocyte enhancer factor-2C phosphorylation levels through integrin-linked kinase in goat skeletal muscle satellite cells. *Cell Biology International*, **39**(11): 1264−1273.

Xie C, Tammi MT. 2009. CNV-seq, a new method to detect copy number variation using high-throughput sequencing. *BMC Bioinformatics*, **10**: 80.

Xiong Q, Tao H, Zhang N, et al. 2020. Skin transcriptome profiles associated with black- and white-coated regions in Boer and Macheng black crossbred goats. *Genomics*, **112**(2): 1853−1860.

Xu ZJ, Wang XW, Zhang ZJ, et al. 2020. Copy number variation of *CADM2* gene revealed its association with growth traits across Chinese *Capra*

hircus (goat) populations. *Gene*, **741**: 144519.

Yang BG, Yuan Y, Zhou DK, et al. 2021. Genome-wide selection signal analysis of Australian Boer goat reveals artificial selection imprinting on candidate genes related to muscle development. *Animal Genetics*, **52**(4): 550−555.

Yin H, Price F, Rudnicki MA. 2013. Satellite cells and the muscle stem cell niche. *Physiological Reviews*, **93**(1): 23−67.

Yin HD, Zhao J, He HR, et al. 2020. Gga-miR-3525 targets *PDLIM3* through the MAPK signaling pathway to regulate the proliferation and differentiation of skeletal muscle satellite cells. *International Journal of Molecular Sciences*, **21**(15): 5573.

Zhang PP, Liang XR, Shan TZ, et al. 2015. mTOR is necessary for proper satellite cell activity and skeletal muscle regeneration. *Biochemical and Biophysical Research Communications*, **463**(1–2): 102–108.

Zhang WY, Zhang SX, Xu YY, et al. 2019. The DNA methylation status of wnt and Tgfβ signals is a key factor on functional regulation of skeletal muscle satellite cell development. *Frontiers in Genetics*, **10**: 220.

Zhang X, Liu L, Chen C, et al. 2013. Interferon regulatory factor-1 together with reactive oxygen species promotes the acceleration of cell cycle progression by up-regulating the cyclin E and CDK2 genes during high glucose-induced proliferation of vascular smooth muscle cells. *Cardiovascular Diabetology*, **12**: 147.

Zhou HH, Chen X, Cai LY, et al. 2019. Erastin reverses ABCB1-mediated docetaxel resistance in ovarian cancer. *Frontiers in Oncology*, **9**: 1398.

Ziegler GC, Almos P, McNeill RV, et al. 2020. Cellular effects and clinical implications of *SLC2A3* copy number variation. *Journal of Cellular Physiology*, **235**(12): 9021−9036.